Antennas Design and Image Reconstruction for Microwave Imaging Systems

André Filipe Lourenço Martins
andre.filipe.lourenco.martins@tecnico.ulisboa.pt

Instituto Superior Técnico, Lisboa, Portugal

April 2018

Abstract

This paper presents the design of a Palm Tree Vivaldi antenna (onwards PTVA) suitable for Microwave Imaging Systems and proposes an Image Reconstruction Algorithm with calibration techniques, based on the Delay and Sum (DAS) algorithm, which aims at detecting intracranial haemorrhages. The prototyped PTVA is a small, compact and thin stucture, offering Ultra Wideband (UWB) characteristics in the 1.61-3.02 GHz frequency band, directive radiation pattern and small reflected pulse distortion. The PTVA features edge slot resonators on its radiators, which are a novel feature used to miniaturize Vivaldi antennas dimensions by confining the electric field, thus creating an increase of the surface current distributions in the resonators, leading to an increased electric length of the antenna. A description of the DAS algorithm is presented and it illustrates the DAS image reconstruction capabilities in the air. By implementing the DAS algorithm, its extention to a more complex scenario is performed, by proposing calibration techniques, the implementation of Fermats Principle and an integration window for a human head model with an haemorrhage. The paper is concluded by performing measurements with the prototyped PTVA and applying the implemented DAS algorithm aiming at detecting a water anomaly, emulating an haemorrhage, inside a human head phantom, with permittivity close to the one found in the human brain.
Keywords: Vivaldi antenna, Delay and Sum Algorithm, Image Reconstruction, Antenna Design, Microwave Imaging Systems

1. Introduction and Motivation

Microwave imaging systems are expected to be affordable, portable and simple to operate [1]. These systems shall be useful in scenarios where a significant dielectric constrast exists, namely in the detection of tumors and haemorrhages. In routine check-up procedures and precocious diagnosis, some of the traditional imaging techniques pose harm or discomfort to patients. For instance, in breast cancer detection women are typically exposed to high doses of ionizing radiation for each mammography, but this procedure is also painful and uncomfortable. A microwave imaging system would allow to perform the examination without pressing the breasts and without using ionizing radiation, since low energy microwave frequencies are harmless to humans. The portable aspect of microwave imaging systems also allows that these systems are deployed in emergency vehicles. In an accident situation, where a traumatic brain injury occurs, intracranial haemorrhage may appear and, the sooner it is detected and treated, the greater the chances of minimizing the issue. Therefore, by equipping emergency vehicles with microwave imaging systems, an examination may be performed when the transportation from the accident location to the hospital is taking place. This way, it is possible to know beforehand if any action is needed towards an intracranial haemorrhage situation upon reaching the hospital or not.

2. State of the Art

The core concept behind a microwave imaging system is a monostatic radar [2]. An antenna emits a signal at a close distance to a target, a human head or breasts for instance, and detects the reflected signals by its different dielectric components. By performing this scan at multiple positions around the target, a set of signals can be obtained and then processed by an imaging algorithm. An image can then be obtained, which highlights the situations where high dielectric contrasts are present, which can be used to detect tumors or hemorrhages. To develop such systems, several obstacles have to be overcomed. While having a simple concept, there are several propagation media, with different permittivity values, ϵ_r. These values depend on the frequency, for instance, at $f = 2.45$ GHz, values of

11.35, 48.83 and 58.18 have been used for bone, brain and blood, respectively, in [3]. The existence of different dielectric boundaries and media not only causes several reflections of the emitted signal, leading to pulse distortion, but also to attenuation in those media, thus making an anomaly detection a difficult process, since the maximum emitted power is also limited [4]. Therefore, developing a suitable antenna is needed in order to correctly detect the anomaly attenuated reflections. While, futurely, this technique is expected to be used in humans, the investigation conducted nowadays must be done using phantoms. A phantom is an object which emulates the electric properties of several tissues of the human body [5], and producing the mixtures needed to do so is also a challenge. Finally, an imaging algorithm developed for this task is not trivial, since it attempts to solve an inverse problem. These problems aim at determining the causal factors that originated a set of observations. In a microwave imaging system problem, the goal of the algorithm is to detect the anomaly which caused the measured reflected signals at the antenna.

2.1. Antennas Design

Since the use of milimiter waves does not pose the dangers of ionizing radiations, their use is desired for medical applications. In particular, for a human head, the microwave spectrum band of 1-3 GHz is suggested, since it offers enough penetration into the tissue . Ideally, the emitted signal should use most of this band, therefore providing the Ultra Wideband (UWB) characteristic, in order to improve signal resolution [2]. As stated previously, a microwave imaging system is expected to be small, portable and cheap, therefore, the antennas must also possess these characteristcs. It is, however, a challenge to develop small antennas for the lower frequencies of the 1-3 GHz band due to the relation between operating frequency and the radiating elements size. While, for breast cancer detection an immersion medium for the scanning may be used to reduce the antennas size [6], the same methods are not applicable for intracrianal tumor or hemorrhage detection. Quasi-Yagi antennas are the most suitable ones to be developed, due to their easy fabrication process, low cost, compact and lightweight structure [7]. The suggestions presented in the literature vary from electromagnetic horns to monopoles, planar and bowtie antennas, Substrate Integrated Waveguide (SIW) printed antennas [7], dipoles [8] [9] and Vivaldi antennas [10] [6]. Vivaldi antennas are characterised by having a curvilinear geometry from the feeding point to the aperture, on the other end [11]. These antennas are usually designed taking into account the lowest desired frequency of operation, which, in this case, results in a quite large antenna, around the desired wavelength [12]. There are, however, novel designs that allow Vivaldi antennas to be more compact, such as the removal of substrate parts [13], the folding of the metallic layers to the other face of the antenna [14] or even cutting the metallic layer following certain geometries [15]. These strategies aim at lengthening the electrical dimensions of the Vivaldi antenna, while maintaining, or even reducing, its physical size by changing the surface currents distribution behaviour.

2.2. Phantoms

Phantoms are objects that emulate the electric properties of living tissue and they are used to tune medical imaging devices, measure mobile phones Specific Absortion Rate (SAR), among other purposes. Depending on the complexity required, phantoms may be either simple models or more accurate 3D printed ones [5] filled with liquid, semisolid or solid mixtures. In order to determine the permittivities of human tissue, the Cole-Cole model, which is an extension to the simpler Debye Relaxation Model, is used [3], after which the different mixtures may be produced, using materials such as glucose, sodium chloridre, diacetin or di-etyhlene glycol buthyl ether (DGBE).

2.3. Image Reconstruction Algorithms

Sound Navigation And Ranging (SONAR) and Radio Detection And Ranging (RADAR) techniques have widely used after the II World War, and its applications range from military purposes, to air and maritime navigation and meteorology. Altough these techniques are widely used, an algorithm applied to microwave imaging must be simpler and require less computational resources. So, algorithms such as the Delay And Sum (DAS) [16], Delay Multiply And Sum (DMAS) [17] and Kirchoff Migration [18] are preferred to when solving the microwave image reconstruction inverse problem. While the Kirchoff Migration algorithm operates in the frequency domain, the DAS and DMAS are time domain algorithms. The concept behind the DAS and DMAS is the summation of received signals, after a certain delay is introduced, so that they add constructively, resulting in signals with small amplitudes (such as the reflection of an anomaly, for instance) to be distinguishable from background noise and higher ampltidude signals. In order to implement these algorithms, a propagation model for the medium has to be developed [19], based on Fermats Principle [1], which states that light travelling time has to be the minimum between a set of two points, taking into consideration the different media, their permittivities and antenna introduced delays.

3. Palm Tree Vivaldi Antenna

Following the works of [10] and [15], a "Palm Tree Vivaldi" antenna (PTVA) was designed in CST. The designed PTVA can be seen in Figures 1 and 2 and its dimensions are seen in Table 1.

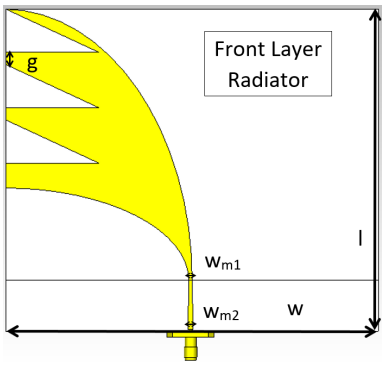

Figure 1: Designed PTVA front view.

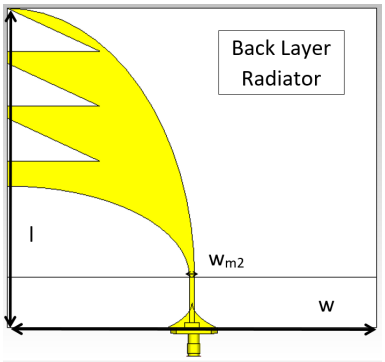

Figure 2: Designed PTVA back view.

Parameter	Value [mm]
w	110
l	95
w_{m1}	1
w_{m2}	1.5
g	3.6

Table 1: PTVA parameters

The designed PTVA was designed on a Rogers RT/Duroid 5880 substrate ($\epsilon_r = 2.2$) and thickness of 0.75 mm. The PTVA presents three edge slot resonators which aim to confine the electric field in these areas (figure 3), thus increasing the surface current distribution there (figure 4). This leads to an increased electric length of the antenna, while keeping its physical dimensions, thus being a useful miniaturization process.

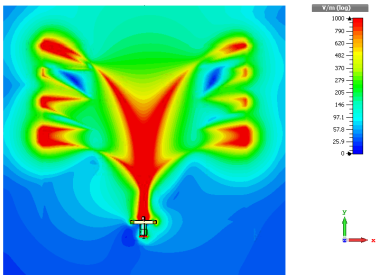

Figure 3: Electric field confinement near the edge slot resonators.

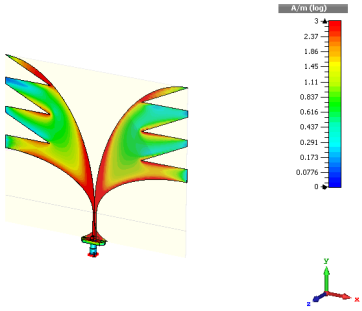

Figure 4: Surface current distribution magnitude.

As referred in the State of the Art, the designed PTVA will ideally operate in the 1-3 GHz frequency band. The S_{11} parameter of the antenna was simulated on CST Studio Suite and, as seen in figure 5, the band of 1.58-2.89 GHz is below the -10 dB threshold, meaning the designed PTVA provides UWB in this frequency range, as intended.

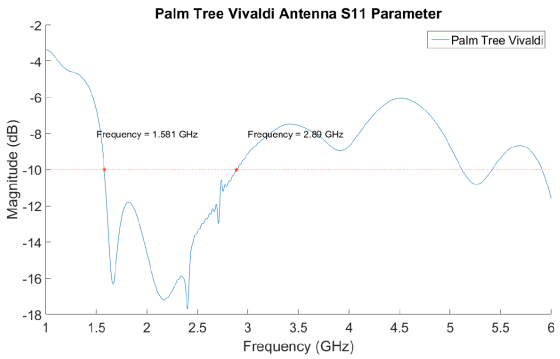

Figure 5: Designed PTVA simulated S_{11} parameter.

While the PTVA is not intended to operate in the farfield region, its radiation pattern is also simulated, in order to illustrate the antenna's capability to illuminate a focused area while scanning a target. The farfield radiation pattern is seen in figure 6.

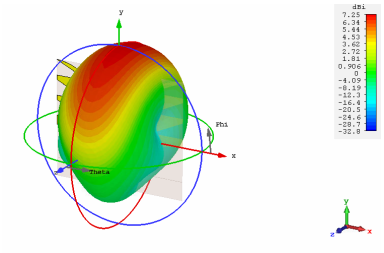

Figure 6: Designed PTVA simulated farfield radiation pattern.

Finally, the designed PTVA pulse distortion must be assessed, since the correct detection of the reflected pulse shape is crucial for image reconstruction algorithms. Therefore, by measuring the S_{11} parameter of the antenna in front of a metal plane, placed at a fixed distance, it is possible to synthesize the reflected signal. By performing this operation, in figure 7 the emitted and received pulse are seen.

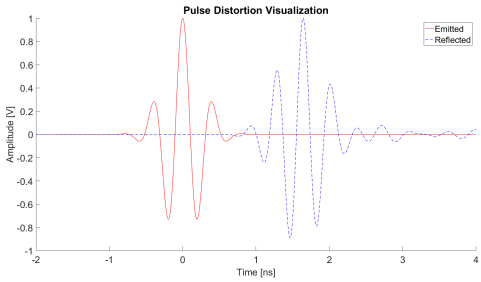

Figure 7: Designed PTVA pulse distortion assessment.

The PTVA introduces small signal distortion, although the pulse shape is easily detectable, making the antenna suitable for a microwave imaging system. The designed PTVA was prototyped with the dimensions presented in Table 1. Its front and back view can be seen in figures 8 and 9.

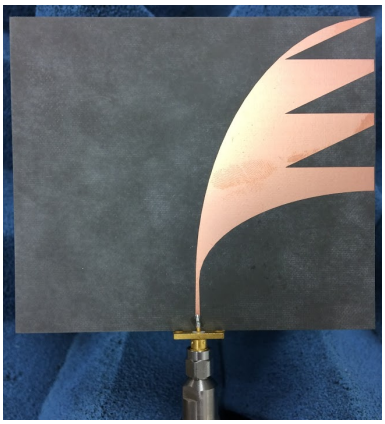

Figure 8: Prototyped PTVA front view.

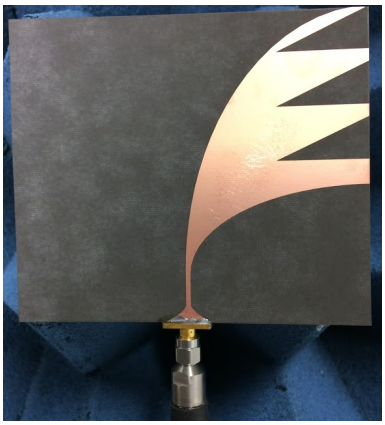

Figure 9: Prototyped PTVA back view.

The prototyped PTVA was connected to a VNA and its S_{11} parameter was measured in free space conditions. As seen in figure 10, the PTVA provides UWB characteristics in the 1.61-3.02 GHz frequency range, with the S_{11} parameter curves following the same behaviour.

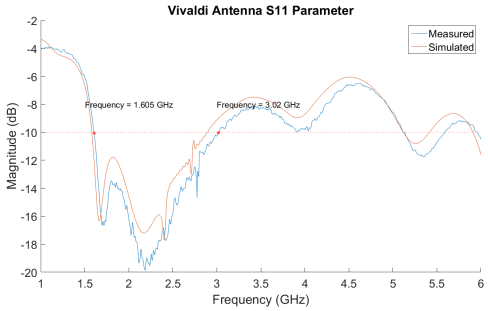

Figure 10: Prototyped PTVA measured S_{11} parameter.

The pulse distortion was also evaluated, by arranging the same measurement setup than the one used in the simulations. As occurred previously, the PTVA introduces small signal distortion, while preserving the pulse shape, making its detection accurate, as seen in figure 11.

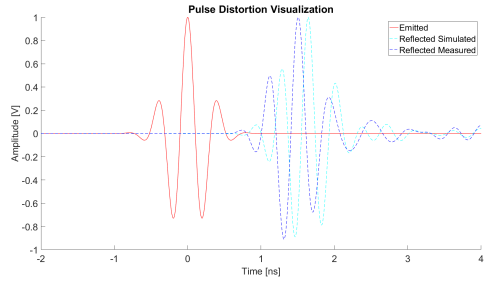

Figure 11: Prototyped PTVA pulse distortion assessment.

4. Image Reconstruction Algorithm

The Delay And Sum (DAS) algorithm was implemented in Matlab in order to perform the Image Reconstruction of a scanning region. The DAS is a time domain algorithm and the computation of the propagation times is fundamental for it to work properly. The DAS, in free space, uses a monostatic radar approach [2] to obtain the reflected signals from a target, with the propagation time being given by equation 1

$$t_p = \frac{(d_1 + d_2) \times \sqrt{\epsilon_r} + d_{ant}}{c} \tag{1}$$

with $d_1 = d_2 = d$ being the distance from the antenna to every point in the scanning region and d_{ant} the propagation delay introduced by the antenna. The distance, d, from the antenna to all points in the scanning region is computed according to expression 2

$$d = \sqrt{(x - a_i)^2 + (y - b_j)^2} \tag{2}$$

and, for a CST Studio Suite simulation set-up which aims at determining the position of a metal target, in the air, for instance the one seen in figure 12,

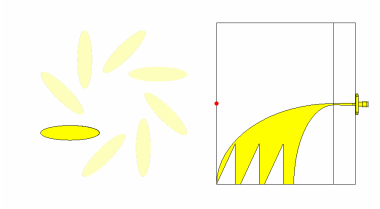

Figure 12: CST Studio Suite simulation model.

in which only one antenna is considered, but 8 target positions are evaluated, a procedure which produces the same effect as considering a circular array of 8 antennas around the target. The reflected signals for the 8 hypothetical antenna positions were synthesized using the simulated S_{11} parameter values, and are seen in figure 13

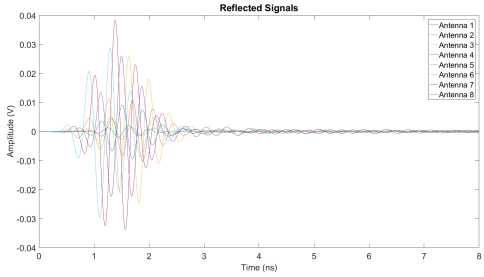

Figure 13: Reflected signals for each antenna position.

and, by applying expressions 1 and 2 to compute the propagation time, it is possible to describe the DAS algorithm with equation 3

$$I(x, y) = \sum_{pos=1}^{N} g(pos) \tag{3}$$

with $g(pos)$ being defined as

$$g(pos) = \begin{bmatrix} a_1b_1 & a_1b_2 & \dots & a_1b_j \\ a_2b_1 & \dots & \dots & \dots \\ \dots & \dots & \dots & a_{i-1}b_j \\ a_ib_1 & \dots & a_ib_{j-1} & a_ib_j \end{bmatrix}$$

and each a_ib_j defined with expression 4

$$a_ib_j = y_r(t) \tag{4}$$

with $y_r(t)$ being the reflected signal on each antenna and t computed according to expression 5

$$t = \frac{d_{ant} + 2\sqrt{(x - a_i)^2 + (y - b_j)^2}}{c} \tag{5}$$

which produces the image, by representing the squared value of the summed amplitude signals seen in figure 14,

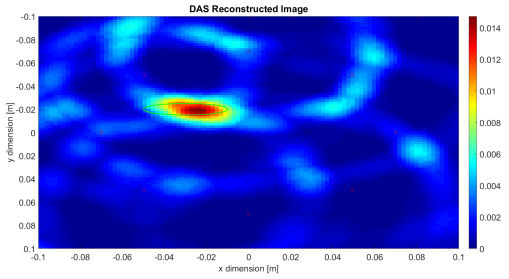

Figure 14: DAS image reconstruction for a copper target, in the air, with squared values of the amplitudes.

which shows a clear detection of the target, in its correct position, as seen by the darker red colours. By extending the propagation model in free space to the one of a human head, two additional propagation media must be considered, the bone ($\epsilon_r = 11$) and brain ($\epsilon_r = 49$). A model of a human head, with a water anomaly emulating an haemorrhage, was designed in CST Studio Suite, as seen in figure 15

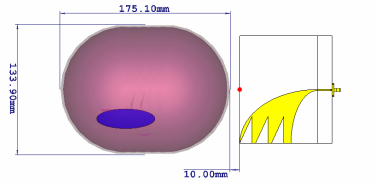

Figure 15: Simulation set-up, as seen in CST Studio Suite, with Human Head model and water anomaly.

The model was, has it was done previously, rotated in 8 positions to emulate the existence of 8 antennas. The reflected signals were synthesized after simulating the S_{11} parameter for each position, as seen in figure 16

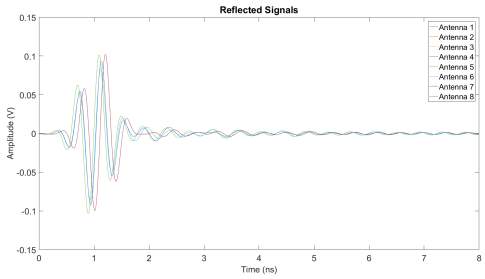

Figure 16: Reflected signals for each antenna position.

in which is clear the existence of a strong reflection from the air/bone dielectric boundary. This reflection has to be eliminated in order to allow the anomaly reflection to be detectable. For this to be feasible, the human skull symmetries have to be used, with a definition of the furthest signals from the anomaly being used, in which all other signals will be aligned with. This calibration is described mathematically as

$$u_{cal}(t) = y_r^*(t - \Delta t) \tag{6}$$

with $u_{cal}(t)$ being the calibration signal, which is the furthest signal from the anomaly, $y_r^*(t - \Delta t)$ aligned to the closest,

$$y_{cal}(t) = y_r(t) - u_{cal}(t) \tag{7}$$

and $y_{cal}(t)$ the signal without the reflection from the air/bone interface. These signals are then calibrated in respect to their symmetric ones, following expression 8

$$y_i(t) = \begin{cases} y_i(t) - y_{i+N/2}(t) & i \leq N/2 \\ y_i(t) - y_{i-N/2}(t) & otherwise \end{cases} \tag{8}$$

resulting in the detection of the anomaly reflection, as seen in figure 17

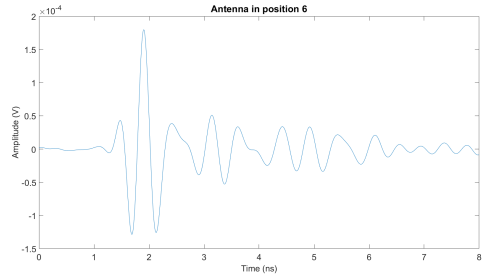

Figure 17: Anomaly reflection detection, after calibration, in antenna in position 6.

and then, in order to eliminate the appearence of a signal in phase oposition, the signal with highest peak amplitude is considered the signal closer to the anomaly, while the other is chopped with zeros until the peak occurence time added with the impulse width, a process described by expression 9

$$y^*(t) = \begin{cases} 0 & t \leq t_p + \tau \\ y^*(t) & t > t_p + \tau \end{cases} \tag{9}$$

In order to accurately represent the human head, a cubic spline interpolation is used, by computing the distances travelled in free space by the reflected signals seen in figure 16, to define a delimiting curve of the air/bone interface. Since it was considered a fixed value for the bone thickness, in figure 18 it is possible to see the bone/brain delimiting curve.

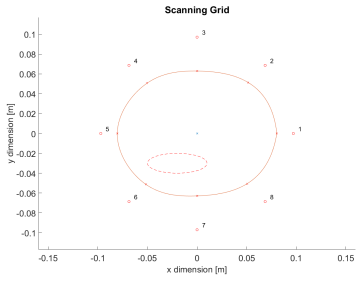

Figure 18: Delimiting curve of the bone/brain dielectric boundary.

Then, by having all points of this curve, it is possible to introduce Fermat's Principle into the image reconstruction algorithm, by considering more than possible path from each antenna to every point in the scanning region, using the one that computes the mininum distance,

$$d_{brain} = d_{min} = min\sqrt{(\alpha_i - a_i)^2 + (\beta_j - b_j)^2} \tag{10}$$

and, using expression 10 and the known permittivity of the brain, it is possible to compute the total propagation time,

$$t_{brain} = \frac{2d_{brain}\sqrt{\epsilon_r}}{c} \tag{11}$$

$$t = t_{air} + t_{bone} + t_{brain} \tag{12}$$

It is then possible to repeat the summation process described by equation 3 to produce the reconstructed image from figure 19, in which the anomaly is detected by the darker colours.

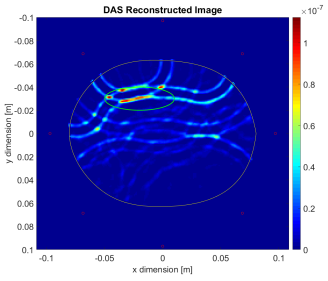

Figure 19: DAS image reconstruction for a water anomaly, inside a human head model, with squared values of the amplitudes.

In order to aid in the detection of the anomaly due to resolution problems with microwaves, an integration window was implemented, described by expression 13

$$a_i b_j = \int_{t_p-\Delta t}^{t_p+\Delta t} y(t)dt \tag{13}$$

which highligths the detection, allowing a more clear visualization of the anomaly, as seen in figure 20

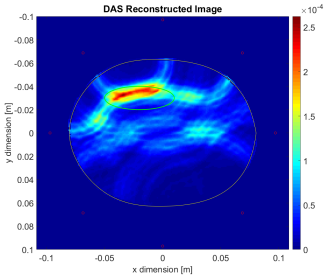

Figure 20: DAS image reconstruction for a water anomaly, inside a human head model, applying the integration window, with squared values of the amplitude.

The developed DAS algorithm was tested using a human head phantom, with a liquid phantom being produced using 68% distilled water, 32% Triton X-100 and 4.4 g/L of sodium chloridre, according to [20], resulting in a liquid with measured permittivity $\epsilon_r = 45.45$ at $f = 2.3$ GHz. A plastic tube containing tap water was inserted into a real sized human skull model, made of polyurethane with measured permittivity $\epsilon_r = 2.75$. The prototyped PTVA was placed in the same horizontal plane as the water anomaly, 1.7 cm below the reference line and 1 cm away from the head phantom in their closest point, which was filled with liquid until the orange dashed line, as seen in figure 21

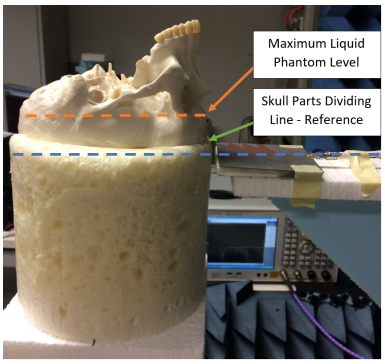

Figure 21: Reference line, position of the antenna 1.7 cm below it and maximum liquid phantom level.

Using this measurement set-up the S_{11} parameter was measured for 8 positions of the antenna, with the reflected signals being used to sucessfully recreate the air/bone delimiting curve, as seen in figure 22

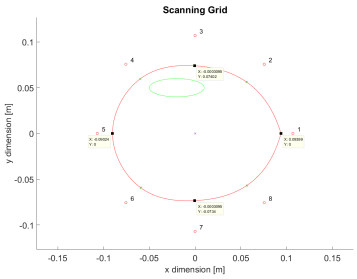

Figure 22: Delimiting curve of the air/bone dielectric boundary.

although failing to calibrate successfully the antennas, leaving air/bone reflections which outshine the water anomaly detection, as seen in figure 23

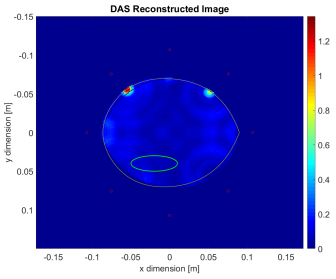

Figure 23: DAS image reconstruction for the human head phantom, with faulty calibration.

In order to detect the haemorrhage emulating structure, a calibration consisting in the subtraction of the S_{11} parameters measured with and without the anomaly was used, resulting in a clear detection, as seen in figure 24, altough some symmetries appear in respect to the $y = 0$ axis, which may be

due to multipath phenomena and reflections on the air/liquid phantom dielectric boundary and due to the implemented DAS only considering a 2D scanning region.

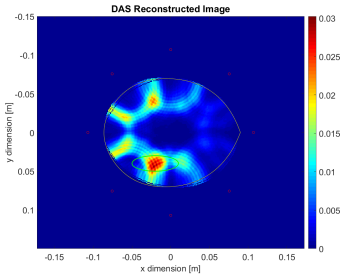

Figure 24: DAS image reconstruction for the human head phantom, using an alternative calibration method.

5. Conclusions

following the literature review which provided the foundaments and knowledge to carry this task, the "Palm Tree Vivaldi" antenna was prototyped. Starting with the requirements desired for an antenna suitable for a microwave imaging system, a basic antipodal Vivaldi antenna and novel features in Vivaldi antennas, the PTVA was designed. By adjusting the Base Vivaldi antenna dimensions and feeding structure, most of the desired frequency band of operation was achieved, with the antenna exhibiting a directive radiation pattern and small pulse distortion. The introduction of the edge slot resonators in the Vivaldi antenna (now called PTVA) radiators allowed to confine the electric field, thus increasing the surface current distribution in these locations, leading to an increase of the electric lenght of the antenna. This increase allowed the PTVA operating frequency band lower limit to decrease, therefore occupying more of the sought 1-3 GHz frequency band. Not only this was achieved, but also the electric lenght increase of the antenna allows its miniaturization, since it is possible to maintain the performance with the introduction of the resonators and reduce the antenna's size. With this in mind, the designed PTVA antenna exhibits the desired UWB characteristic in the band of 1.58-2.89 GHz band, low pulse distortion and directive properties. This is achieved in a miniaturized design, in a compact and thin structure. The PTVA was then prototyped, with the fabricated antenna showing the same S_{11} behaviour as the simulations, achieving UWB in the 1.61-3.02 GHz, occupying most of the 1-3 GHz band, and preserving the desired properties observed in the simulations. The antenna was successfully prototyped and tested, and fulfils the requirements needed for a Microwave Imaging System. Following the antenna design chapter of this dissertation, the imaging algorithm is adressed. After a conceptual illustration of the Delay and Sum algorithm, simulations using CST Studio Suite are conducted, using the designed PTVA model. After a successful demonstration of the DAS reconstructing a scanning environment composed of a metal target in the air, a propagation model for the human head is proposed and designed in CST Studio Suite. By simulating the developed model, calibration strategies are proposed to overcome the air/bone dielectric boundary and detect the signal reflected from a water anomaly, which emulates an haemorrhage. Following the proposed calibration description, Fermat's Principle was taken into account in the DAS algorithm propagation times computation. Finally, after correctly detecting the anomaly, an integration window was implemented to further improve its highlight, improving image resolution. All this was achieved with the DAS algorithm running in an acceptable computation time. With the simulations results being positive, it was decided to build a phantom and perform measurements with the prototyped PTVA. Using a polyurethane human skull model as container, producing a liquid phantom and fabricating a water anomaly, which emulates an haemorrhage, measurements were perfomed in laboratory. Not only the S_{11} parameter measurements, required for the image reconstruction process, were conducted, but also measurements to determine solid and liquid materials permittivity accurately. While, using the proposed calibration methods, the anomaly could not be detected, the use of different calibration method allowed to perform its detection. This calibration consisted in measuring the S_{11} parameter with the anomaly and then subtracting the S_{11} parameter without it. The described procedure made the removal of the air/bone reflections possible and allowed to demonstrate the DAS detection capabilities, highlighting the haemorrhage emulating structure in its location. As future work, several topics are left open for reasearch work. For instance, the aditional miniaturization of Vivaldi antennas, while keeping the working band in the 1-3 GHz interval, is desired. The effect of different edge slot resonator shapes and orientations on the electric lenght increase of the antenna and its miniaturization possibilities is crucial to have smaller antennas deployed in a real world scenario. Moreover, aditional miniaturization strategies are suggested to be researched. The biggest challenge in microwave image reconstruction is, undoubtedly, the artifact removal calibrations. In this work, the proposed calibration failed when accounting laboratory measurements, and investigation on overcoming the biggest reflections from the first dielectric boundary are suggested to take place. In fact, calibration techniques or signal processing methods in-

vestigation is suggested in order to solve the hardest challenge in microwave imaging systems. The extension of the DAS algorithm to a 3D scanning environment is also a path of investigation, since it should allow more accurate propagation times estimations, due to more paths to the anomalies being considered. Further improvements on the existing algorithms, either in the time or frequency domain, are also suggested, aiming at improving image resolution and accuracy.

Acknowledgements
I would like to thank Prof. António Topa for inspiring me and guiding through the Telecommunications area, Mr. Carlos Brito and Mr. António Almeida for providing the technical expertise needed during this work, João Felício for all the patience and time spent explaining new concepts and providing ideas and solutions to overcome several problems that appeared. To Prof. Carlos Fernandes and Prof. António Moreira I express my most sincere gratitude for challenging me with this Thesis, for the friendly relation we shared during this time and for all the fantastic feedback and words of wisdom and advice that made this Thesis possible. To all my dear friends who were always there for me. To Anaísa, my girlfriend, for all the hours spent by my side, cheering for me, for all the love and support, giving everything humanly possible to make these months of work definitely better. Finally, I would like to thank my caring parents and grandparents. Even with the distance and by spending so much time far away from them, their kind words of wisdom and support came to me everyday. They made this journey possible, they made it a unique experience, they made me who I am, and I can't ever thank them enough for all the sacrifices made in order for me to pursue this goal of my life.

References

[1] A. Mobashsher, A. Mahmoud, and A. M.Abbosh, "Portable Wideband Microwave Imaging System for Intracranial Hemorrhage Detection Using Improved Back-Projection Algorithm with Model of Effective Head Permittivity," *Sci. Rep. 6*, no. 20459, 2016.

[2] B. J. Mohammed, A. M. Abbosh, S. Mustafa, and D. Ireland, "Microwave System for Head Imaging," *IEEE Trans. Instrum. Meas.*, vol. 63, pp. 117–124, January 2014.

[3] P. S. Hall and Y. Hao, *Antennas and Propagation for Body-Centric Wireless Communications*, ch. 2. Electromagnetic Properties and Modeling of the Human Body, pp. 11–20. Artech House, 2006.

[4] Federal Communications Commission, "Specific Absorption Rate SAR for Cellular Telephones."

[5] A. T. Mobashsher and A. M. Abbosh, "Three-Dimensional Human Head Phantom with Realistic Electrical Properties and Anatomy," *IEEE Antennas Wireless Propag. Lett.*, vol. 13, pp. 1401–1404, 2014.

[6] J. Bourqui, M. Okoniewski, and E. C. Fear, "Balanced Antipodal Vivaldi Antenna with Dielectric Director for Near-Field Microwave Imaging," *IEEE Trans. Antennas Propag.*, vol. 58, no. 7, pp. 2318–2326, 2010.

[7] S. Lin, S. Yang, A. E. Fathy, and A. Elsherbini, "Development of a Novel UWB Vivaldi Antenna Array using SIW Technology," *Progress In Electromagnetic Research*, vol. 90, pp. 369–34, 2009.

[8] A. T. Mobashsher and A. M. Abbosh, "Slot-Loaded Folded Dipole Antenna with Wideband and Unidirectional Performance for L-Band Applications," *IEEE Antennas Wireless Propag. Lett*, vol. 13, pp. 798–801, 2014.

[9] A. T. Mobashsher and A. M. Abbosh, "Compact 3-D Slot-Loaded Folded Dipole Antenna with Unidirectional Radiation and Low Impulse Distortion for Head Imaging Applications," *IEEE Trans. Antennas Propag.*, vol. 64, pp. 3245–3250, July 2016.

[10] A. M. Abbosh, "Directive Antenna for Ultrawideband Medical Imaging Systems," *Int. J. of Antennas and Propag.*, 2008.

[11] N. Hamzah and K. A. Othman, "Designing Vivaldi Antenna with Various Sizes using CST Software," *Proc. of the World Congr. on Eng.*, vol. 2, July 2011.

[12] Y.-W. Wang, G.-M. Wang, and B.-F. Zong, "Directivity Improvement of Vivaldi Antenna Using Double-Slot Structure," *IEEE Antennas Wireless Propag. Lett.*, vol. 12, pp. 1380–1383, 2013.

[13] J. Kowalewski, U. Dey, T. Mahler, and T. Zwick, "Vivaldi Antenna with Improved Directivity for Medical Applications," *German Microwave Conference*, pp. 123–128, March 2015.

[14] K. Kikuta and A. Hirose, "Compact Folded-Fin Tapered Slot Antenna for UWB Applications," *IEEE Antennas Wireless Propag. Lett.*, vol. 14, pp. 1192–1195, 2014.

[15] A. M. D. Oliveira, M. B. Perotoni, S. T. Kofuji, and J. F. Justo, "A Palm Tree Antipodal Vivaldi Antenna With Exponential Slot Edge for Improved Radiation Pattern," *IEEE Antennas Wireless Propag. Lett.*, vol. 14, pp. 1334–1337, 2015.

[16] K. E. Thomenius, "Evolution of Ultrasound Beamformers," *Proc. of the IEEE Int. Ultrasounds Symp.*, pp. 1615–1622, September 1996.

[17] G. Matrone, A. S. Savoia, G. Caliano, and G. Magenes, "The Delay Multiply and Sum Beamforming Algorithm in Ultrasound B-Mode Medical Imaging," *IEEE Trans. Med. Imag.*, vol. 34, pp. 940–949, April 2015.

[18] X. Zhuge, T. Savelyev, A. Yarovoy, L. Ligthart, and B. Levitas, "Comparison of Different Migration Techniques for UWB Short-Range Imaging," *Proceedings of the 6th European Radar Conference*, pp. 184–187, September 2009.

[19] A. T. Mobashsher, A. M. Abbosh, and Y. Wang, "Microwave System to Detect Traumatic Brain Injuries Using Compact Unidirectional Antenna and Wideband Transceiver with Verification on Realistic Head Phantom," *IEEE Trans. Microw. Theory Tech.*, vol. 62, pp. 1862–1836, September 2014.

[20] N. Joachimowicz, C. Conessa, T. Henriksson, and B. Duchêne, "Breast phantoms for microwave imaging," *IEEE Antennas Wirel. Propag. Lett.*, vol. 13, pp. 1333–1336, 2014.